

Cite this article as: Burris NS, Nordsletten DA, Sotelo JA, Grogan-Kaylor R, Houben IB, Figueroa CA *et al.* False lumen ejection fraction predicts growth in type B aortic dissection: preliminary results. *Eur J Cardiothorac Surg* 2019; doi:10.1093/ejcts/ezz343.

False lumen ejection fraction predicts growth in type B aortic dissection: preliminary results

Nicholas S. Burris ^{a,*}, David A. Nordsletten^{b,c}, Julio A. Sotelo ^{d,e,f}, Ross Grogan-Kaylor ^a,
Ignas B. Houben ^b, C. Alberto Figueroa ^{c,g}, Sergio Uribe ^{d,f,h} and Himanshu J. Patel^b

^a Department of Radiology, University of Michigan, Ann Arbor, MI, USA

^b Department of Cardiac Surgery, University of Michigan, Ann Arbor, MI, USA

^c Department of Biomedical Engineering, University of Michigan, Ann Arbor, MI, USA

^d Biomedical Imaging Center, Pontificia Universidad Católica de Chile, Santiago, Chile

^e Department of Electrical Engineering, Pontificia Universidad Católica de Chile, Santiago, Chile

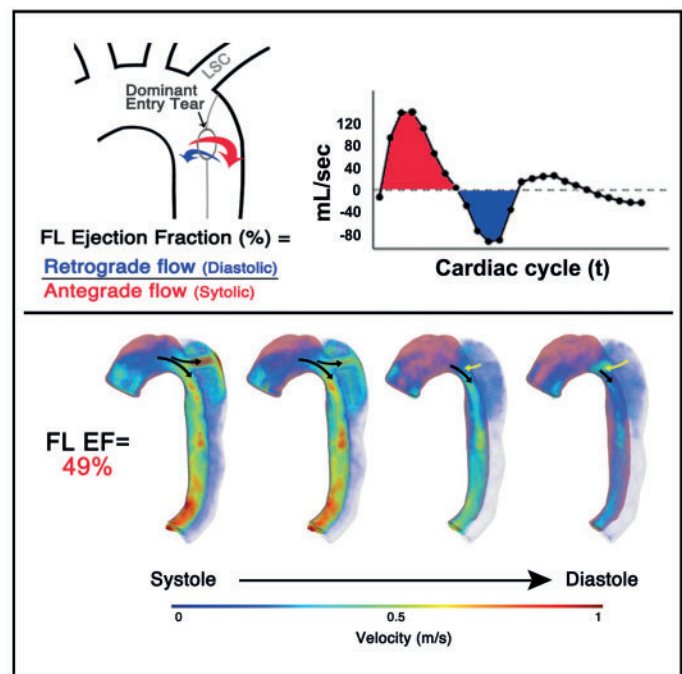
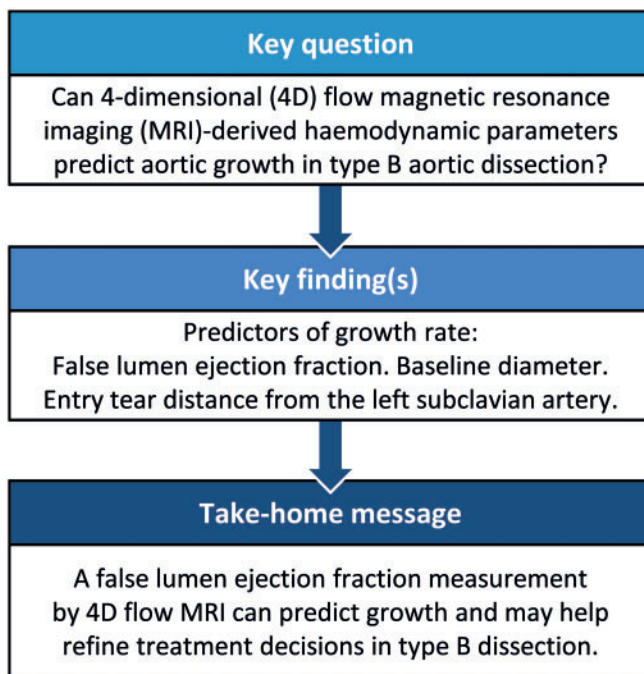
^f Millennium Nucleus for Cardiovascular Magnetic Resonance, Santiago, Chile

^g Department of Surgery, University of Michigan, Ann Arbor, MI, USA

^h Department of Radiology, School of Medicine, Pontificia Universidad Católica de Chile, Santiago, Chile

* Corresponding author. Department of Radiology, University of Michigan, 1500 E. Medical Center Drive, Cardiovascular Center 5588, SPC-5030, Ann Arbor, MI 48109-5030, USA. Tel: +1 734-763-7169; e-mail: nburris@med.umich.edu (N.S. Burris).

Received 16 September 2019; received in revised form 6 November 2019; accepted 13 November 2019



Abstract

OBJECTIVES: Current risk assessment strategies in type B aortic dissection are focused on anatomic parameters, although haemodynamic abnormalities that result in false lumen (FL) pressurization are thought to play a significant role in aortic growth. The objective of this study was to evaluate blood flow of the FL using 4D flow magnetic resonance imaging (MRI) and identify haemodynamic and anatomic factors that independently predict the rate of aortic growth.

Presented at the 33rd Annual Meeting of the European Association for Cardio-Thoracic Surgery, Lisbon, Portugal, 3–5 October 2019.

METHODS: Patients with dissection of the descending thoraco-abdominal aorta ($n=18$) were enrolled in a prospective observational study and underwent 4D flow MRI for haemodynamic assessment of the entry tear and FL. Anatomic parameters were obtained by magnetic resonance angiography and baseline computed tomography. False lumen ejection fraction (FL EF) was defined the ratio of retrograde flow rate at the dominant entry tear during diastole over the antegrade systolic flow rate.

RESULTS: The median aortic growth rate was 3.5 mm/year (interquartile range 0.5–8.1 mm/year). Entry tear peak velocity was lower in patients with enlarging aortic dimensions (95.5 ± 24.1 vs 128.1 ± 37.4 cm/s, $P=0.039$). After adjusting for co-variables FL EF ($\beta=0.15$, $P=0.004$), baseline maximal aortic diameter ($\beta=0.37$, $P=0.001$) and the entry tear distance from the left subclavian artery ($\beta=0.07$, $P=0.016$) were significant predictors of aortic growth rate.

CONCLUSIONS: Beyond standard anatomic risk factors, FL EF is an independent predictor of aortic growth rate and may represent an intuitive, non-invasive method to estimate FL pressurization and improve patient-specific risk assessment in patients with type B aortic dissection.

Keywords: Type B aortic dissection • False lumen • Computed tomography angiography • 4D flow magnetic resonance imaging • Aneurysm

ABBREVIATIONS

CI	Confidence interval
CT	Computed tomography
FL EF	False lumen ejection fraction
FL	False lumen
LSC	Left subclavian artery
MRA	Magnetic resonance angiography
MRI	Magnetic resonance imaging
SD	Standard deviation
TBAD	Type B aortic dissection
TEVAR	Thoracic endovascular aortic repair
TL	True lumen
vWERP	Virtual work-energy relative pressure

INTRODUCTION

Aneurysmal degeneration of the false lumen (FL) is the most common long-term complication in type B aortic dissection (TBAD), occurring in ~75% of patients who are medically managed [1]. Prophylactic thoracic endovascular aortic repair (TEVAR) has been shown to promote aortic remodelling, slow disease progression and decrease long-term aorta-specific mortality [2, 3]. However, TEVAR for uncomplicated TBAD remains a debated topic, given concerns of excess cost and procedural complications. Thus, there remains a significant need for methods to better risk-stratify patients with TBAD to allow for a targeted repair strategy. Existing methods for estimating the risk in TBAD focus on anatomic variables measured on computed tomography (CT) images, which are limited in their ability to capture the complex and dynamic character of aortic dissection [4–6]. A recent CT-based risk prediction analysis showed that including estimated FL outflow improved the model's predictive power from ~0.55 to 0.7, further stressing the importance of FL haemodynamic assessment of the FL [4].

Haemodynamic forces are thought to play a significant role in the development of aneurysm in TBAD, and thus TEVAR exerts its protective effects by decreasing the FL inflow and promoting thrombosis. Unfortunately, haemodynamics of the FL are poorly evaluated using standard CT images, and invasive catheter-based measurements of FL pressure are rarely performed in clinical practice. Studies using both computation modelling and flow phantoms techniques have demonstrated that FL pressurization

occurs in the setting of excess inflow relative to outflow, resulting in higher mean diastolic and pulse pressure in the FL [7–9]. Furthermore, in the setting of insufficient outflow, the degree of retrograde flow increases in proportion to the degree of outflow insufficiency [7, 10].

Time-resolved 3-dimensional phase-contrast magnetic resonance imaging (MRI) (4D flow) is an advanced MRI technique that allows for volumetric assessment of blood flow in large vessels [11]. 4D flow MRI studies in TBAD have identified a variety of abnormal blood flow characteristics in the FL that may relate to the risk of future FL aneurysm formation, although the mechanisms that link blood flow abnormalities and aortic growth remain poorly defined [12, 13]. Retrograde flow (or diastolic flow reversal) may be an intuitive marker of FL pressurization that can be easily identified by 4D flow MRI [14]. Specifically, the proportion of FL flow exiting at the dominant entry tear in a retrograde fashion during diastole, which in this manuscript will be referred to as the 'false lumen ejection fraction' (FL EF), has been proposed as surrogate maker of FL pressurization and has been shown to be elevated among chronic TBAD patients with a history of progressive FL growth [13]. Despite the simplicity of the FL EF metric, the haemodynamic environment of the FL is complex and influenced by a variety of patient-specific factors such as anatomy and age of the dissection, highlighting the need for a multivariate analysis to control for the effects of confounding relationships between variables.

The purpose of this study was to perform a comprehensive analysis of FL haemodynamics in a cohort of patients with chronic TBAD and to further evaluate the ability of a variety of haemodynamic variables to independently predict aortic growth rate during follow-up. We hypothesize that the degree of blood exiting the FL through the dominant entry tear during diastole (FL EF) will independently predict growth of the dissected descending thoraco-abdominal aorta.

MATERIALS AND METHODS

Patient identification and clinical characteristics

Between November 2014 and August 2019, a total of 18 adult patients with unrepaired, chronic dissection of the descending thoracic aorta ($n=15$ type B; $n=3$ repaired type A with residual tear in the descending thoracic aorta) were prospectively enrolled in an observational, IRB-approved study

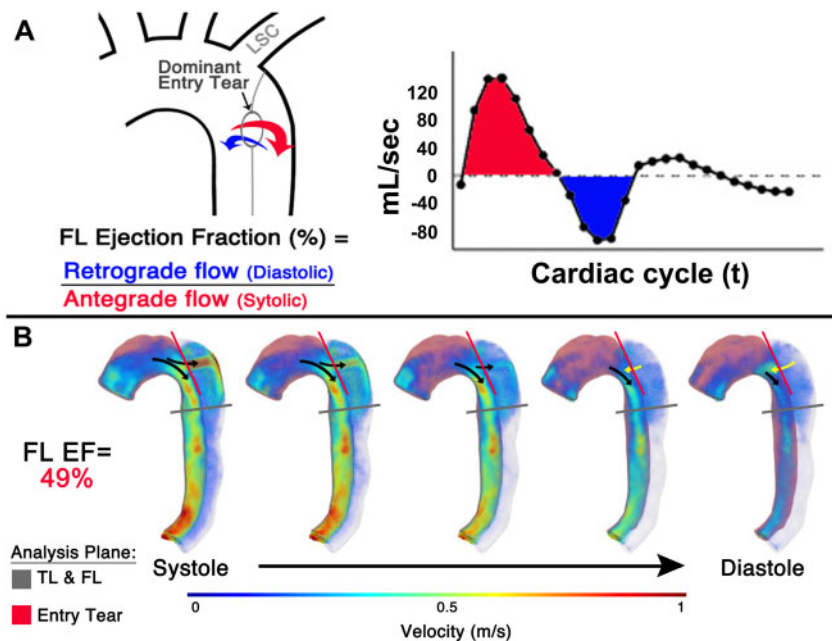


Figure 1: 4D flow haemodynamic assessment. The FL EF was measured in the plane of the dominant entry tear and was defined as the proportion of retrograde flow (l/min) exiting the FL during diastole over the systolic antegrade flow volume (l/min) at the dominant entry tear (**A**). Three-dimensional visualization of 4D flow magnetic resonance imaging data in a patient with type B aortic dissection demonstrating the flow analysis plane for the entry tear FL EF measurement (**B**, red line) and the TL and FL analysis planes (**B**, grey line) measured 3 cm distal to the tear. Antegrade flow is depicted in the TL and FL during systole (black arrow, **B**), with retrograde flow being 'ejected' from the FL during diastole (yellow arrow, **B**) in a representative case with measured FL EF of 57%. FL: false lumen; FL EF: false lumen ejection fraction; LSC: left subclavian artery; TL: true lumen.

(HUM00120679) and underwent a single research MRI exam. TBAD patients were identified through our Cardiac Surgery clinic ($n=95$) and were excluded for: (i) complete FL thrombosis ($n=7$), (ii) entry tear location in the abdominal aorta ($n=3$), (iii) symptoms of chest pain or evidence of malperfusion ($n=3$), (iv) claustrophobia or other contraindication to MRI ($n=22$), (v) estimated glomerular filtration rate <30 ml/min/1.73 m² ($n=8$), and 28 patients declined participation. Patient information was collected by a combination of research questionnaire and chart review. Baseline anatomic data including maximal diameter (including aortic wall), true lumen (TL) and FL size, distance of the entry tear from the left subclavian artery (LSC), FL location and branch vessel anatomy were measured on the baseline clinical CT scan acquired at the time of aortic dissection diagnosis using clinical image analysis software using a centreline approach (Vitrea, Vital Images, Toshiba, Tokyo, Japan).

Magnetic resonance imaging technique and imaging analysis

All MRI exams were performed on 3T MRI scanners ($n=4$: MR750, GE Medical Systems, Milwaukee, WI, USA; $n=14$: Ingenia, Philips, Best, Netherlands). The research MRI examination included breath-hold, contrast-enhanced magnetic resonance angiography (MRA), reconstructed at 0.9 mm³ isotropic resolution after the administration of an iron-based MRI contrast agent (ferumoxytol, 3 mg/kg) in 12 patients at 3 mg/kg dose or gadobenate dimeglumine (Multihance[®]; Bracco, Milano, Italy) in 5 patients at 0.2 ml/kg dose. Following the MRA, 4D flow MRI was performed covering the thoracic aorta. Briefly, 4D flow scan parameters included: flip angle=15°, reconstructed resolution = ~1.5 mm × 1.5 mm × 2.5 mm, acceleration factor = 2.0 × 2.0, views-per-segment = 3, average scan

time = 11 min, and average temporal resolution = 47 ms, velocity encoding value = 200 cm/s. Raw 4D flow MRI data were uploaded to a web-based software application (Arterys, San Francisco, CA, USA) for data reconstruction, visualization and flow analysis. Segmentations of the TL and FL were generated with dedicated software (Mimics, Materialise, Leuven, Belgium) and additional 4D flow haemodynamic analysis was performed in a computational framework based on finite-elements developed in MATLAB (MathWorks, Natick, MA, USA) [15, 16]. Visualization of 4D flow data was performed using ParaView (Kitware Inc., Clifton Park, NY, USA).

Aortic growth rate was calculated as the difference in maximal aortic diameter between the baseline CT angiography and the research MRA over the time interval. Subjects were categorized as 'stable' if their aortic growth rate was <3 mm/year and 'enlarging' if aortic growth rate was ≥ 3 mm/year, based on the reported mean growth rate in TBAD and known variability in diameter measurements [17]. Dominant entry tear was defined as the tear with the highest measured rate of inflow into the FL. FL EF (previously termed entry tear regurgitant fraction) was calculated from 4D flow MRI data by placing a flow analysis region of interest in the plane and location of the dominant entry tear, and was defined as the ratio of retrograde diastolic flow rate (l/min) over the antegrade systolic flow rate (l/min) measured in the plane of dominant entry tear as further illustrated in Fig. 1. Haemodynamics were also assessed in planes orthogonal to the direction of flow in the proximal TL and FL at 3 cm distal to the entry tear.

Statistical analysis

Patient characteristics were reported as mean ± standard deviation (SD) for continuous variables, and frequencies for

Table 1: Patient and anatomic characteristics

Characteristics	Overall (n = 18)	Stable (n = 8)	Enlarging (n = 10)	P-value
Patient age (years), mean \pm SD	52.1 \pm 9.5 (range 31–71)	47.5 \pm 8.3	55.8 \pm 9.2	0.064
Dissection type				
Repaired type A, n (%)	3 (17)	3 (37)	0 (0)	
Type B, n (%)	15 (83)	5 (63)	10 (100)	0.069
Sex (male/female), n	13/5	6/2	7/3	1.000
Connective tissue disease, n (%)	3 (17)	2 (25)	1 (10)	0.559
Hypertension, n (%)	16 (89)	6 (75)	10 (100)	0.183
Smoking history, n (%)	9 (50)	5 (63)	4 (40%)	0.637
Age of dissection (years), mean \pm SD	3.7 \pm 3.2 (range 0.2–8.0)	5.7 \pm 3.2	2.1 \pm 2.1	0.013
Aortic growth rate (mm/year), median (IQR)	3.5 (0.5–8.1) (range 0–22)	0.3 (0–2.1)	7.9 (5.8–12.4)	0.001 ^a
Maximum diameter at MRI (mm), mean \pm SD	46.3 \pm 8.6 (range 32–62)	40.1 \pm 7.1	50.7 \pm 7.3	0.011
Dominant entry tear size by MRI (mm), ^b median (IQR)	16.2 (10.8–20.0) (range 5–44)	13.2 (10.1–24.3)	17.0 (12.3–20.0)	0.594 ^a
Baseline CT anatomic characteristics				
Entry tear distance from LSC (mm), median (IQR)	20.0 (2.0–24.0) (range 0–130)	10.0 (2.0–45.0)	20.0 (19.0–34.0)	0.448 ^a
Inner curvature FL location, n (%)	5 (28)	2 (25)	3 (30)	1.000
Maximal aortic diameter (mm), mean \pm SD	39.4 \pm 7.6 (range 29–58)	38.1 \pm 4.1	40.5 \pm 9.6	0.524
Partial FL thrombus, n (%)	5 (28)	2 (25)	3 (30)	1.000

^aMann–Whitney *U*-test.

^bMean of maximal and minimal tear dimensions.

CT: computed tomography; FL: false lumen; IQR: interquartile range; LSC: left subclavian artery; MRI: magnetic resonance imaging; SD: standard deviation.

categorical variables. Skewness and kurtosis were assessed (sktest in Stata), and continuous variables are reported as mean \pm SD if normally distributed or median (interquartile range) if skewed. Categorical values are reported as *n* (%). Pearson's correlation was used to determine associations between aortic growth rate, anatomic and haemodynamic parameters. Comparison of continuous variables was performed with the unpaired *t*-tests or non-parametric Mann–Whitney *U*-test, and a *P*-value of <0.05 was considered significant. Fisher's exact test was used to evaluate difference in frequency of categorical variables. Pairwise correlation matrices were used to identify multicollinearity amongst predictors. Subsequently, parsimonious multiple linear regression models with Huber/White/sandwich robust variance estimator were used to identify independent predictors of aortic growth rate amongst a group of potential anatomic and haemodynamic variables described in prior publications [6, 12, 13]. Statistical analyses were performed using Stata 14.0 (StataCorp LP, College Station, TX, USA).

RESULTS

Patient characteristics

The average patient age was 52.1 \pm 9.5 years and the majority of patients were male (13/18, 72%). The vast majority of patients had a history of hypertension (16/18, 89%) and the minority had an established history of connective tissue disease (3/18, 17%). The average age of the dissection at the time of the research MRI was 3.71 \pm 3.17 years (range 0.24–8.01 years). The mean baseline aortic diameter based on index CT was 39.4 \pm 7.6 mm (range 29–58 mm) and the maximal aortic diameter at the time of the research MRI was 46.3 \pm 8.6 mm (range 32–62 mm). The median aortic growth rate between baseline CT and research MRI was 3.5 mm/year (interquartile range 0.5–8.1 mm/year, range 0–22 mm/year). The median entry tear size was 16.2 mm (interquartile range 10.8–20.0 mm, range 5–44 mm). Baseline aortic

diameter, entry tear size and distance of the entry tear from the LSC were not significantly different between patients with stable and enlarging aortic dimensions. These data are shown in greater detail in Table 1.

Haemodynamic assessment

The average net flow rate in the TL was higher than the FL (3.1 \pm 1.1 vs 1.4 \pm 1.3 l/min) as was the TL peak velocity (87.3 \pm 34.9 vs 64.5 \pm 30.2 cm/s). Retrograde flow was common in the FL with 16 (89%) of patients demonstrating measurable retrograde flow in the FL during diastole. Conversely, flow in the TL was almost exclusively antegrade with only 5 (27%) patients demonstrating any measurable TL retrograde flow with the highest degree of retrograde flow in the TL being only 5% by volume vs 89% in the FL. The mean FL EF was 28.9 \pm 24.4% (range 0–88%), and FL EF did not correlate well with the FL retrograde flow fraction measured 3 cm distal to the primary tear ($r=0.13$, $P=0.607$). FL EF was significantly elevated in patients with enlarging vs stable aortic dimensions (43.8 \pm 22.1% vs 10.3 \pm 10.1%, $P=0.001$). Entry tear peak velocity was lower in patients with enlarging aortic dimensions (95.5 \pm 24.1 vs 128.1 \pm 37.4 cm/s, $P=0.394$). Haemodynamic parameters are summarized in greater detail in Table 2 and 2 representative cases are shown in Fig. 2.

Bivariate and multivariate analysis of aortic growth

FL EF demonstrated a moderate–strong correlation with aortic growth rate ($r=0.71$, $P=0.001$) and baseline maximal aortic diameter demonstrated a weak–moderate ($r=0.42$, $P=0.081$) but non-significant correlation with aortic growth. Dominant entry tear size ($r=0.01$, $P=0.999$), distance of the entry tear from the LSC ($r=0.27$, $P=0.286$), FL peak velocity ($r=-0.1$, $P=0.731$), FL net flow ($r=0.36$, $P=0.139$) and FL retrograde flow fraction ($r=0.31$, $P=0.217$) did not significantly correlate with aortic growth rate on bivariate analysis. There was no significant

Table 2: 4D flow haemodynamic parameters

Characteristics	Overall (n = 18)	Stable (n = 8)	Enlarging (n = 10)	P-value
True lumen^a				
Net flow (l/min), median (IQR)	2.6 (2.2–4.0) (range 2.0–5.5)	2.4 (2.1–2.8)	2.9 (2.5–4.4)	0.051 ^b
Peak velocity (cm/s), median (IQR)	87.1 (69.5–96.0) (range 37–169)	87.1 (77.6–89.6)	89.2 (54.0–99.7)	0.790 ^b
False lumen^a				
Net flow (l/min), median (IQR)	1.1 (0.4–2.0) (range 0.1–4.6)	1.5 (0.4–3.5)	0.8 (0.4–1.9)	0.477 ^b
Peak velocity (cm/s), mean ± SD	64.5 ± 30.2 (range 16–120)	64.9 ± 34.5	64.2 ± 28.1	0.96
Retrograde flow fraction (%), mean ± SD	33.4 ± 31.9 (range 0–89)	24.2 ± 31.5	40.9 ± 31.9	0.28
Systolic flow eccentricity, mean ± SD	0.22 ± 0.7 (range 0.10–0.33)	0.22 ± 0.6	0.22 ± 0.9	0.97
Dominant entry tear				
Net flow (l/min), median (IQR)	0.7 (0.4–0.9) (range 0.1–4.6)	0.8 (0.4–2.7)	0.6 (0.2–0.8)	0.168 ^b
Peak velocity (cm/s), mean ± SD	110.0 ± 34.1 (range 66–199)	128.1 ± 37.4	95.5 ± 24.1	0.04
False lumen ejection fraction (%) (retrograde flow fraction), mean ± SD	28.9 ± 24.4 (range 0–88)	10.3 ± 10.1	43.8 ± 22.1	0.001

^aMeasured 3 cm distal to dominant entry tear.

^bMann–Whitney U-test.

IQR: interquartile range; SD: standard deviation.

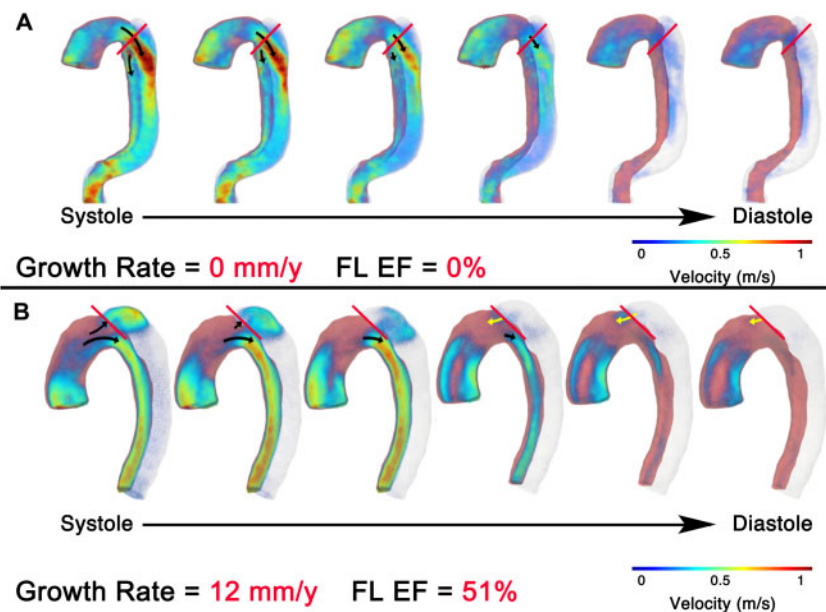


Figure 2: Representative case examples. A 52-year-old patient with type B aortic dissection and baseline maximal diameter of 42 mm that remained unchanged at 1-year follow-up computed tomography exam, with a large proximal entry tear (32 mm), but similar-sized re-entry tear at the coeliac origin, and a measured FL EF of 0% (A). A 60-year-old man with type B aortic dissection and baseline maximal diameter of 50 mm that grew to 54 mm over a 4-month period, with a 20-mm proximal entry tear just beyond the origin of the left subclavian artery with measured FL EF of 51% (B). FL EF: false lumen ejection fraction.

correlation between FL EF and entry tear size ($r=0.01$, $P=0.949$). Scatter plots of several of these correlations are shown in Fig. 3.

Multiple linear regression analysis models were performed to identify independent predictors of aortic growth rate amongst a group of anatomic and haemodynamic variables of interest. After adjusting for co-variables, the variables that were independently associated with aortic growth rate were FL EF [$\beta=0.15$, 95% confidence interval (CI) 0.07–0.23; $P=0.001$], baseline maximal aortic diameter ($\beta=0.37$, 95% CI 0.18–0.56; $P=0.001$), and the entry tear distance from the LSC ($\beta=0.07$, SE 0.02, 95% CI 0.02–0.12; $P=0.016$), with the overall model adjusted $R^2=0.87$ (Table 3). The significance of predictors in the regression model did not change when patients with connective tissue disease (Supplementary Material, Table S1) or repaired type-A dissection and connective tissue disease (Supplementary Material, Table S2) were excluded.

DISCUSSION

The key observations of this study can be summarized as follows: (i) 4D flow MRI is a useful method for quantifying the complex blood flow patterns in the FL of patients with chronic TBAD, (ii) peak velocity at the entry tear jet is lower in patients with a history of enlarging FL, likely due to obstructed or insufficient FL outflow, (iii) FL EF, defined as the proportion of retrograde diastolic flow at the entry tear, demonstrates a moderate–strong correlation with aortic growth rate and (iv) after adjustment for co-variables, FL EF, baseline maximal diameter and distance of the entry tear from the LSC are independent predictors of aortic growth rate.

The results of our study are largely in agreement with prior literature on this topic. Specifically, baseline maximal diameter and distance of the entry tear from the LSC are commonly reported

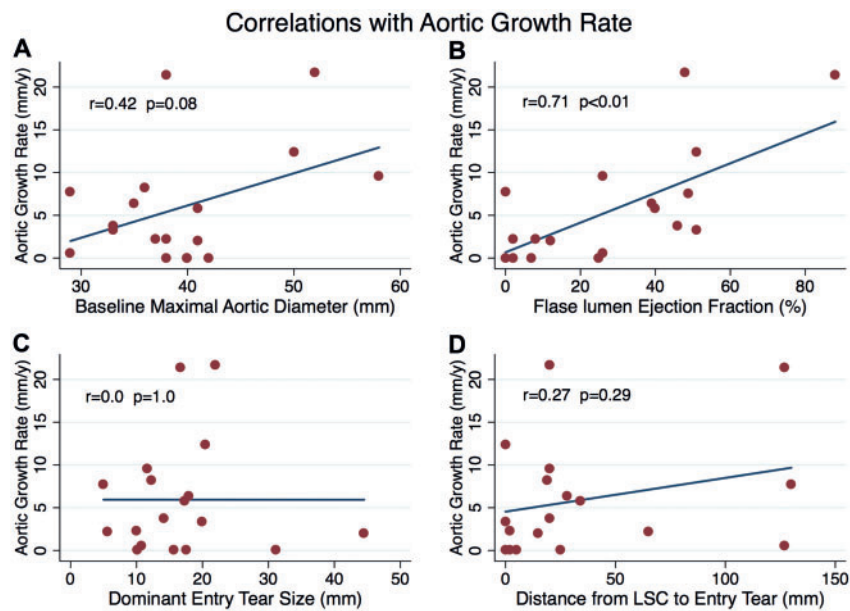


Figure 3: Scatter plots demonstrating the correlations between aortic growth rate baseline maximal aortic diameter (A), false lumen ejection fraction (B), dominant entry tear size (C) and distance from the LSC to the entry tear (D). LSC: left subclavian artery.

Table 3: Multivariate regression—predictors of aortic growth rate

Characteristics	β Coefficient	95% CI	P-value
False lumen ejection fraction	0.15	0.07–0.23	0.001
Baseline maximal aortic diameter	0.37	0.18–0.56	0.001
Interval ²	-0.11	-0.28 to 0.07	0.205
Dominant entry tear size	0.21	-0.12 to 0.53	0.184
False lumen net flow	-1.50	-3.45 to 0.44	0.116
False lumen peak velocity	0.04	-0.03 to 0.11	0.262
Entry tear distance from left subclavian	0.07	0.02–0.12	0.016

Adjusted $R^2 = 0.87$.

CI: confidence interval.

as predictors of aortic growth and are widely recognized as risk factors for aneurysmal degeneration and other adverse events [6]. Additionally, our observation that bi-phasic flow and retrograde/regurgitant flow is common in the FL has also been well described using a variety of imaging and computational modelling techniques [7, 10, 13, 14, 18, 19]. Lastly, data from the International Registry of Aortic Dissection (IRAD) have shown that partial FL thrombosis is an independent predictor of mortality in TBAD patients and hypothesized that this was related to FL pressurization due to FL outflow obstruction [20]. Interestingly, while FL peak velocity, net flow and flow eccentricity have been previously reported to be associated with aortic growth by Clough *et al.* [12], we did not observe such associations in analyses.

Current treatment algorithms are largely based baseline diameter, given that diameter has a clear relationship with wall stress, risk of aneurysm formation and other complications. However, FL pressurization also plays a role in promoting growth and other outcomes in TBAD. A recent study of 83 patients with acute, uncomplicated TBAD found that decreased FL outflow (as predicted from CT branch vessel anatomy) was a significant predictor of

adverse events, an effect that is likely attributable to insufficient outflow leading to FL pressurization [4, 7]. However, FL pressurization is a difficult phenomenon to assess in clinical practice using available non-invasive imaging techniques, and while branch vessel anatomy based on CT can be used to estimate the relative amount of FL outflow, without a method to assess FL inflow, the degree of inflow–outflow imbalance that leads to FL pressurization cannot be reliably determined. Computational modelling techniques have been applied to study FL haemodynamics, and while such highly controlled experimental studies are critical for isolating the haemodynamics effects of tear size, tear location and other anatomic features, they are currently limited for the routine assessment of clinical patients due to their time-consuming nature, the difficulty of accurately accounting for the effects of small tears and a variety of assumptions about the wall thickness/elasticity and flap motion [7, 21]. However, recent developments in 4D flow MRI-based techniques that utilize work-energy methods virtual work-energy relative pressure (vWERP) allow for relative pressure mapping across any vascular segment in clinically applicable timeframes, and has been used to assess bicuspid aortic valve and aortic haemodynamics, and may be useful for the non-invasive assessment of FL relative pressure gradients [22–24].

Measurement of FL EF by 4D flow MRI may avoid many of the limitations of CT and computational modelling, and while 4D flow does not directly yield FL pressure measurements, the quantification of retrograde diastolic flow at the entry tear may be a method to estimate FL pressurization non-invasively. Furthermore, considering that TBAD anatomy can be complex, and that distal re-entry pathways are more frequently small and difficult to define by non-invasive imaging, the fact that FL EF measured is based on the dominant entry tear—which is almost always clearly identifiable—avoids the challenges of directly measuring FL outflow. Furthermore, as FL EF reflects a ratio of flow rates, its measurement is less susceptible to errors related to image artefacts and other technical factors than more advanced 4D flow parameters, and 4D flow assessment of flow rate in

TBAD has shown excellent reproducibility [25]. In practice, 4D flow imaging can be acquired immediately following a standard MRA, and in addition assessing FL pressurization can help identify secondary entry/re-entry tears that may guide endovascular repair planning [26].

Limitations

Our study has 3 main limitations. First, the study cohort is relatively small and recruited from a high-volume aortic referral centre, so there is potential for bias. However, given that 4D flow in aortic dissection is a relatively understudied topic, to our knowledge, this 18-patient cohort represents the largest 4D flow evaluation of TBAD patients to date. Second, our cohort is composed of chronic dissections. Given the timing of 4D flow imaging, it is possible that elevated FL EF is a result of aortic growth rather than a cause. However, we think this is unlikely, given that the mechanism of in-flow-outflow imbalance leading to FL pressurization has been supported by Sailer *et al.* using CT images from acute dissection patients, as well as in computational and flow phantom studies [4, 7, 9]. Continued research by our group will focus on enrolment of acute TBAD patients. Lastly, while the popularity of 4D flow MRI continues to rise, given significant decreases in scan time and the availability of commercial postprocessing software, it remains a technique that is used for clinical assessment in only a small number of specialized centres, thus limiting the generalizability of our findings. However, despite this limitation, we believe that our findings provide further support for the importance of FL haemodynamics in the risk assessment of TBAD patients.

In an era of increasing rates of TEVAR for treatment of TBAD, there is a significant need for methods to identify high-risk patients to allow for early targeted repair. In addition to standard anatomic assessments, a more comprehensive risk-stratification strategy would ideally include an assessment of FL pressurization such as that afforded by measurement of FL EF. With continued research and validation of FL EF as a predictor of aortic growth and other outcomes, we envision a future MRI-based approach to assess TBAD patients that will allow for a combined assessment of standard anatomic parameters in addition to haemodynamic markers of FL pressurization to help better predict patient risk.

SUPPLEMENTARY MATERIAL

Supplementary material is available at *EJCTS* online.

ACKNOWLEDGEMENTS

The authors would like to acknowledge Bo Yang, Karen Kim, Shinichi Fukuhara and G. Michael Deeb, UM Cardiovascular Health Improvement Project (CHIP) team members, and clinical coordinators Mary Passow, Lynn Hendee, Susan Hooker and Maureen Daly for their assistance with patient enrolment, as well as our research MRI staff including James Pool, Ladonna Austin, Suzan Lowe and James O'Conner for their assistance with enrolment and research MRI examinations.

Funding

This work was supported by the Radiologic Society of North America Research Scholar Grant [RSCH1801] to N.S.B; Millennium

Science Initiative of the Ministry of Economy, Development and Tourism, grant Nucleus for Cardiovascular Magnetic Resonance, and CONICYT–FONDECYT [#1181057] and FONDECYT [#1180832] and CONICYT–FONDECYT Postdoctorado 2017 [#3170737] to J.A.S. and S.U; Engineering and Physical Sciences Research Council [EP/N011554/1 and EP/R003866/1] to D.A.N; and Joe D. Morris Collegiate Professorship, Phil Jenkins Breakthrough Fund and David Hamilton Fund in Cardiac Surgery to H.J.P.

Conflict of interest: none declared.

Author contributions

Nicholas S. Burris: Conceptualization; Data curation; Formal analysis; Funding acquisition; Investigation; Methodology; Project administration; Resources; Software; Supervision; Validation; Visualization; Writing—original draft; Writing—review & editing. **David A. Nordsletten:** Data curation; Formal analysis; Investigation; Methodology; Project administration; Resources; Supervision; Validation; Visualization; Writing—review & editing. **Julio A. Sotelo:** Data curation; Formal analysis; Investigation; Methodology; Resources; Software; Supervision; Validation; Visualization; Writing—original draft; Writing—review & editing. **Ross Grogan-Kaylor:** Data curation; Formal analysis; Investigation; Methodology; Software; Validation; Visualization; Writing—review & editing. **Ignas B. Houben:** Conceptualization; Formal analysis; Investigation; Methodology; Resources; Software; Writing—review & editing. **C. Alberto Figueroa:** Conceptualization; Formal analysis; Investigation; Methodology; Project administration; Resources; Software; Supervision; Validation; Writing—review & editing. **Sergio Uribe:** Data curation; Formal analysis; Investigation; Project administration; Resources; Software; Supervision; Visualization; Writing—review & editing. **Himanshu J. Patel:** Conceptualization; Data curation; Formal analysis; Funding acquisition; Investigation; Methodology; Project administration; Resources; Supervision; Validation; Visualization; Writing—review & editing.

REFERENCES

- [1] Fattori R, Montgomery D, Lovato L, Kische S, Di Eusanio M, Ince H *et al.* Survival after endovascular therapy in patients with type B aortic dissection: a report from the International Registry of Acute Aortic Dissection (IRAD). *JACC Cardiovasc Interv* 2013;6: 876–82.
- [2] Nienaber CA, Kische S, Rousseau H, Eggebrecht H, Rehders TC, Kundt G *et al.* Endovascular repair of type B aortic dissection: long-term results of the randomized investigation of stent grafts in aortic dissection trial. *Circ Cardiovasc Interv* 2013;6:407–16.
- [3] Iannuzzi JC, Stapleton SM, Bababekov YJ, Chang D, Lancaster RT, Conrad MF *et al.* Favorable impact of thoracic endovascular aortic repair on survival of patients with acute uncomplicated type B aortic dissection. *J Vasc Surg* 2018;68:1649–55.
- [4] Sailer AM, van Kuijk SM, Nelemans PJ, Chin AS, Kino A, Huininga M *et al.* Computed tomography imaging features in acute uncomplicated Stanford type-B aortic dissection predict late adverse events. *Circ Cardiovasc Imaging* 2017;10:e005709.
- [5] Schwartz SI, Durham C, Clouse WD, Patel VI, Lancaster RT, Cambria RP *et al.* Predictors of late aortic intervention in patients with medically treated type B aortic dissection. *J Vasc Surg* 2018;67:78–84.
- [6] Spinelli D, Benedetto F, Donato R, Piffaretti G, Marrocco-Trischitta MM, Patel HJ *et al.* Current evidence in predictors of aortic growth and events in acute type B aortic dissection. *J Vasc Surg* 2018;68: 1925–35.e8.
- [7] Rudenick PA, Segers P, Pineda V, Cuellar H, Garcia-Dorado D, Evangelista A *et al.* False lumen flow patterns and their relation with morphological and biomechanical characteristics of chronic aortic dissections. Computational model compared with magnetic resonance imaging measurements. *PLoS One* 2017;12:e0170888.
- [8] Tsai TT, Schlicht MS, Khanafer K, Bull JL, Valassis DT, Williams DM *et al.* Tear size and location impacts false lumen pressure in an ex vivo model of chronic type B aortic dissection. *J Vasc Surg* 2008;47:844–51.

- [9] Canchi S, Guo X, Phillips M, Berwick Z, Kratzberg J, Krieger J *et al.* Role of re-entry tears on the dynamics of type B dissection flap. *Ann Biomed Eng* 2018;46:186–96.
- [10] Birjiniuk J, Timmins LH, Young M, Leshnowar BG, Oshinski JN, Ku DN *et al.* Pulsatile flow leads to intimal flap motion and flow reversal in an in vitro model of type B aortic dissection. *Cardiovasc Eng Tech* 2017;8:378–89.
- [11] Burris NS, Hope MD. 4D flow MRI applications for aortic disease. *Magn Reson Imaging Clin N Am* 2015;23:15–23.
- [12] Clough RE, Waltham M, Giese D, Taylor PR, Schaeffter T. A new imaging method for assessment of aortic dissection using four-dimensional phase contrast magnetic resonance imaging. *J Vasc Surg* 2012;55:914–23.
- [13] Burris NS, Patel HJ, Hope MD. Retrograde flow in the false lumen: marker of a false lumen under stress? *J Thorac Cardiovasc Surg* 2019;157:488–91.
- [14] Francois CJ, Markl M, Schiebler ML, Niespodzany E, Landgraf BR, Schlensak C *et al.* Four-dimensional, flow-sensitive magnetic resonance imaging of blood flow patterns in thoracic aortic dissections. *J Thorac Cardiovasc Surg* 2013;145:1359–66.
- [15] Sotelo J, Dux-Santoy L, Guala A, Rodriguez-Palomares J, Evangelista A, Sing-Long C *et al.* 3D axial and circumferential wall shear stress from 4D flow MRI data using a finite element method and a Laplacian approach. *Magn Reson Med* 2018;79:2816–23.
- [16] Sotelo J, Urbina J, Valverde I, Mura J, Tejos C, Irarrazaval P *et al.* Three-dimensional quantification of vorticity and helicity from 3D cine PC-MRI using finite-element interpolations. *Magn Reson Med* 2018;79:541–53.
- [17] Sueyoshi E, Sakamoto I, Hayashi K, Yamaguchi T, Imada T. Growth rate of aortic diameter in patients with type B aortic dissection during the chronic phase. *Circulation* 2004;110:II-256–61.
- [18] Karmonik C, Muller-Eschner M, Partovi S, Geisbusch P, Ganten MK, Bismuth J *et al.* Computational fluid dynamics investigation of chronic aortic dissection hemodynamics versus normal aorta. *Vasc Endovascular Surg* 2013;47:625–31.
- [19] Cheng Z, Juli C, Wood NB, Gibbs RG, Xu XY. Predicting flow in aortic dissection: comparison of computational model with PC-MRI velocity measurements. *Med Eng Phys* 2014;36:1176–84.
- [20] Tsai TT, Evangelista A, Nienaber CA, Myrmet T, Meinhardt G, Cooper JV *et al.* Partial thrombosis of the false lumen in patients with acute type B aortic dissection. *N Engl J Med* 2007;357:349–59.
- [21] Dillon-Murphy D, Noorani A, Nordsletten D, Figueroa CA. Multi-modality image-based computational analysis of haemodynamics in aortic dissection. *Biomech Model Mechanobiol* 2016;15:857–76.
- [22] Donati F, Myerson S, Bissell MM, Smith NP, Neubauer S, Monaghan MJ *et al.* Beyond Bernoulli: improving the accuracy and precision of noninvasive estimation of peak pressure drops. *Circ Cardiovasc Imaging* 2017;10:e005207.
- [23] Lamata P, Pitcher A, Krittian S, Nordsletten D, Bissell MM, Cassar T *et al.* Aortic relative pressure components derived from four-dimensional flow cardiovascular magnetic resonance. *Magn Reson Med* 2013;72:1162–9.
- [24] Marlevi D, Ruijsink B, Balmus M, Dillon-Murphy D, Fovargue D, Pushparajah K *et al.* Estimation of cardiovascular relative pressure using virtual work-energy. *Sci Rep* 2019;9:1375.
- [25] de Beaufort HW, Shah DJ, Patel AP, Jackson MS, Spinelli D, Yang EY *et al.* Four-dimensional flow cardiovascular magnetic resonance in aortic dissection: assessment in an ex vivo model and preliminary clinical experience. *J Thorac Cardiovasc Surg* 2019;157:467–76.e1.
- [26] Allen BD, Aouad PJ, Burris NS, Rahsepar AA, Jarvis KB, Francois CJ *et al.* Detection and hemodynamic evaluation of flap fenestrations in type B aortic dissection with 4D flow MRI: comparison with conventional MRI and CT angiography. *Radiol Cardiothorac Imaging* 2019;1:[Epub ahead of print].